

# Application Note

## Automatic Localization of Mono- to N-Layers of 2D Materials by Spectroscopic Imaging Ellipsometry

SEBASTIAN FUNKE

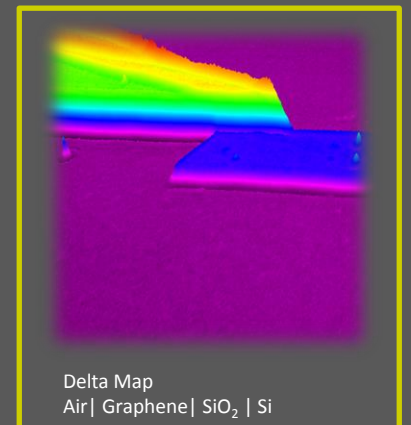
[www accurion.com](http://www accurion.com)

**Contact:**

**S. Funke**

[sfu@accurion.com](mailto:sfu@accurion.com)

Accurion GmbH,  
Stresemannstrasse 30,  
D-37079 Göttingen, Germany,  
[www accurion.com](http://www accurion.com).



# Automatic Localization of Mono- to N-Layers of 2D Materials by Spectroscopic Imaging Ellipsometry

SEBASTIAN FUNKE

[SFu@accurion.com](mailto:SFu@accurion.com)

[www.accurion.com](http://www.accurion.com)

Accurion GmbH, Stresemannstr. 30, 37073 Göttingen

In this application note we present the capability of imaging spectroscopic ellipsometry to automatically localize small flakes down to a few microns in lateral dimension and to distinguish between mono-, bi- or n-layers. The method is based on the pixel-wise comparison of a stack of delta and psi maps with the optical model. In general, it offers the opportunity to identify areas of a sample with defined layer thickness or optical properties. For demonstration purposes, a sample with a graphene flake in-between a number of thicker layers and one with a number of exfoliated Molybdenum disulfide flakes are presented.

## Introduction

The research of A. Geim and K. Novoselov leveraged the mechanical exfoliation of graphene as a new preparation method [1]. Frindt and Yoffe [1963] prepared 2D flakes of Molybdenum Disulfide in a similar way [2]. The first step is the exfoliation, the second the identification of the 2D material in between flakes of layer- and bulk material areas. The state of the art is the exfoliation on a special SiO<sub>2</sub> (300 nm)|Si substrate to enable the localization by the use of a light microscope. This procedure has to be performed manually and the result is strongly related to the skills of the operator. Raman spectra are established as the identification method. Also Raman mapping is an opportunity for the localization, but due to low sensitivity of Raman-scattering, the task is very time consuming.

A new focus in 2D material related research is the characterization of physical properties of layered systems related to the thickness as well as the formation of complex stacks made from different 2D materials. By stacking e.g. graphene and MoS<sub>2</sub> Monolayers the hybrid structures have promising properties for e.g. opto-electronic devices [3]–[6]. Regarding MoS<sub>2</sub> 2D materials the variation in thickness seems to be related to the band gap [7].

To summarize a method is needed, that not only allows the localization and identification of monolayers of 2D materials independent of the substrate but also enables the localization and identification of flakes with a well-defined thickness.



**Figure 1.** EP4 with Polarizer arm on the left and Analyzer arm with the optical system at the right. The sample can be placed onto a motorized xy-table.

In ellipsometry, the ellipsometric angles  $\Delta$  and  $\Psi$  are related to the thickness and the dispersion function of a layered system. Kravets et al. obtained the optical dispersion of mechanically exfoliated Graphene by spectroscopic ellipsometry [8]. The wavelength spectra or the ellipsometric angles at significant wavelength can be understood as a finger print of the required flake. Spectroscopic imaging Ellipsometry permits measurement of  $\Delta$  and  $\Psi$  on tiny regions with the “Region of Interest” concept. Upon decreasing the regions to the size of a pixel, microscopic maps of  $\Delta$  and  $\Psi$  with a lateral resolution down to 1  $\mu\text{m}$  can be obtained.

Matkovic et al. and Wurstbauer et al. showed that imaging ellipsometry is able to characterize the optical properties of small flakes of Graphene [9], [10]. Thermally reduced Graphene was investigated by Jung et al. [11]. Albrektsen et al. reported a thickness map that reveals distinct terraces separated by steps, which have heights corresponding to monolayers or bilayers of graphene [12].

The reported profile show five steps on a distance of 25  $\mu\text{m}$ . In addition, they applied several complementary techniques like optical reflection microscopy, AFM and Raman spectroscopy. The findings of imaging ellipsometry and complementary techniques are in excellent agreement.

## Imaging Ellipsometry

In ellipsometry the ellipsometric angles  $\Delta$  and  $\Psi$  describe the phase shift and the amplitude ratio of the s, and p polarization after the reflection from a sample respectively. To obtain  $\Delta$  and  $\Psi$  a well-defined state of polarization before the reflection from a sample must be provided by a Polarizer (P) and a Compensator. The Analyzer (A) detects the state of polarization after the reflection. By doing nulling ellipsometry the calculation of  $\Delta$  and  $\Psi$  can be directly obtained of the angles of P and A by:

$$\Delta = 2P + \frac{\pi}{2}, \quad \Psi = A.$$

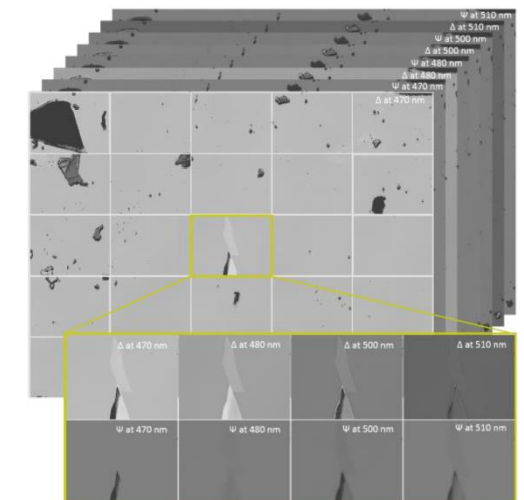


**Figure 2.** Principle of mapstacks with x,y-pattern.

In nulling ellipsometry the compensator is a quarter-wave plate, whereas P and A are linear polarizers. The rotation of P polarizes the incoming light in such way, that the reflected beam is linearly polarized. By rotating A to 90° to the linearly polarized light, minimum intensity at the detector will be observed. A detailed description of the theoretical background on ellipso-metry is given in [13]–[15].

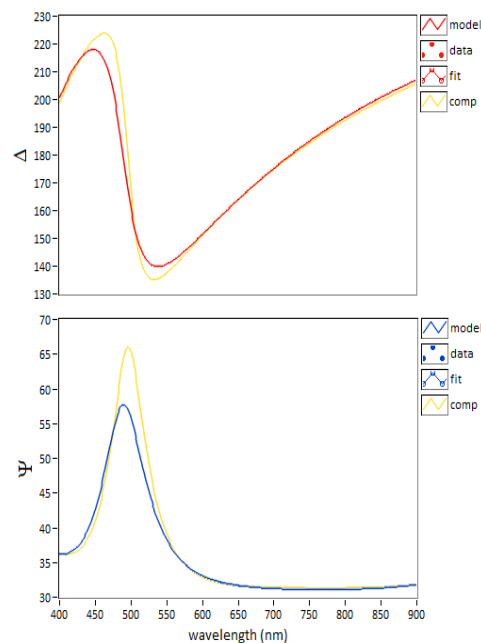


**Figure 4.** (top):  $\Delta$  plot of monolayer (red) and trilayer (orange) of Graphene over the wavelength range as obtained from the EP4Model (bottom):  $\Psi$  plot of monolayer (red) and trilayer (orange) of Graphene over the wavelength range.

For imaging ellipsometry the reflected beam will be guided through a microscopical system through the Analyzer to the detector. Therefore one can obtain  $\Delta$  and  $\Psi$  at every pixel on the detector for the sample area that is in the field of view of the optical system. By changing the wavelength of the monochromatic incoming light, spectroscopic imaging ellipsometry (SIE) can be done. All following measurements are performed with an

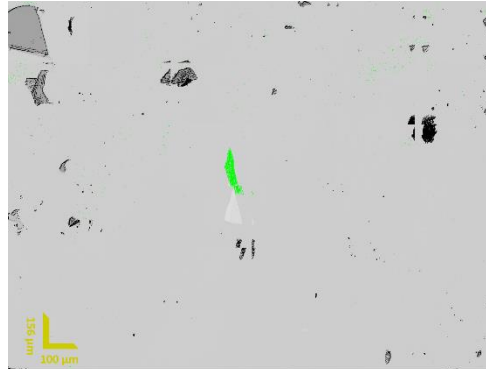


**Figure 3.** An image of monolayer graphene located in a 5x5 xy-pattern. Pixel within a  $\Delta$  and  $\Psi$  range of  $\pm 2.5$  and a threshold of 0.85 are displayed green.

EP4 from Accurion, Göttingen as seen in Figure [1].

### Automatic Localization of Small Flakes

With a motorized xy-table the EP4 is able to automatic pattern a sample. Therefore the user only needs to set the points at the edge of the sample and choose the pattern style. The device will measure with defined parameters maps at every discrete point of the xy-pattern. To locate flakes or areas with a defined thickness, spectroscopic maps at every position are taken. These spectroscopic maps,  $\Delta$  and  $\Psi$  for selected wavelengths, at one position in the pattern will be called a mapstack. For a 5x5 pattern with 4 wavelengths in the measurement parameters 25 mapstacks are obtained. A graphical illustration is shown in Figure 2.

For the automatic localization the dispersion of the sought-after material must be known. In the EP4Model the  $\Delta$  and  $\Psi$  values will be calculated for the desired thickness. For a monolayer of Graphene / MoS<sub>2</sub> a thickness of 0.36nm / 0.63 nm respectively are known. The program *Search for Thickness* takes the  $\Delta/\Psi$  values as reference for the search. In an iterative process the values for  $\Delta$  and  $\Psi$  for every pixel at each wavelength in one mapstack will be compared to the data obtained

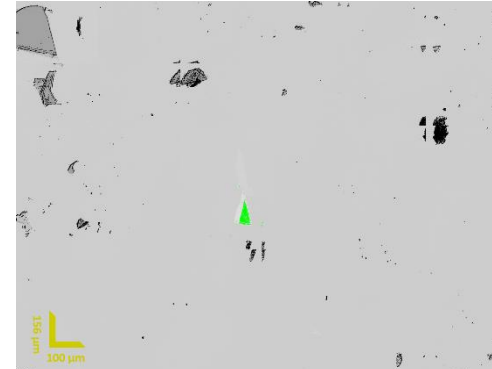


**Figure 5.** Results for the flakesearch of trilayer of graphene on 5x5 pattern with a  $\Delta$  and  $\Psi$  range of  $\pm 2.2$  and a threshold of 0.7.

from the EP4Model. A  $\Delta/\Psi$  plot for a trilayer (orange) and a monolayer of Graphene on a silicon dioxide-silicon substrate is shown in Figure 4. By defining a threshold noisy data can be compensated, especially for small flakes close to the lateral resolution limit of down to 1  $\mu\text{m}$ . **The threshold defines how many percent of the  $\Delta$  and  $\Psi$  values of one pixel compared over the wavelengths in each mapstack need to be in the given range of  $\Delta$  and  $\Psi$  from the model.** Once the pixels that are in the range and in the threshold of the Model values are found, a clustersearch must be done. The clustersearch provides a function to find only the

regions where found pixels are stacked together, e.g. in small flakes or areas of the desired thickness. The user can choose a cluster size of pixel x pixel and another threshold. The algorithm filters the mapstacks and gives out the positions where

$$n_{\text{found}} \geq n_{\text{pixel x}} * n_{\text{pixel y}} * \text{threshold}$$

for each filtercluster is given. So the threshold describes the occurrence of found pixel in the given cluster.

### Results

The result for a flakesearch for 5x5 pattern with 4 wavelengths from 470 nm - 510 nm is shown in Figure 3. The algorithm clearly identifies the monolayer area of the Graphene flake on the silicon-silicon dioxide layer (green pixels). All green pixels in the stitched result window are in the range with the threshold of the modeldata. The flakesearch algorithm finds a flake in mapstack 21 and 22, where the flake is located in the middle of the patterned area. It neglects e.g. dust particles, edge effects may have the same  $\Delta$  and  $\Psi$  variation as the desired layer. For the same measurement a flake search for a trilayer of Graphene was done. The result is shown in Figure 5.

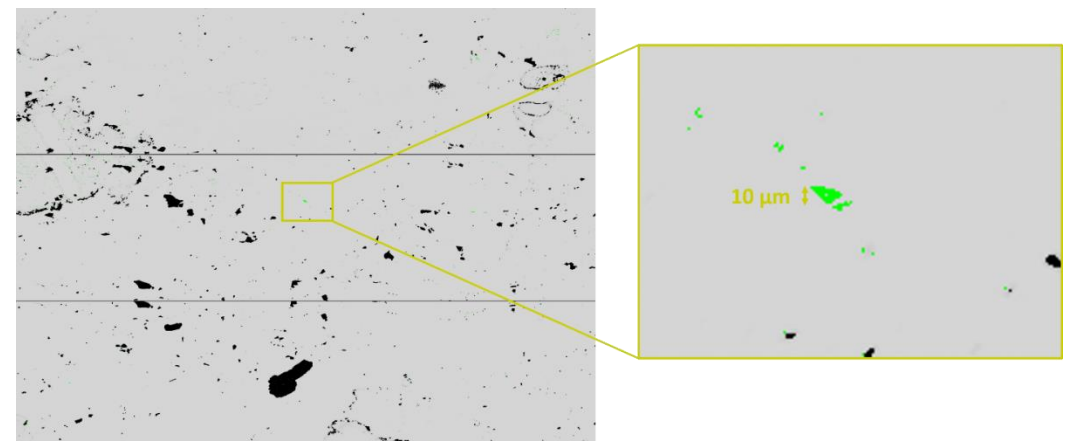


**Figure 6.** Stitched maps with a pixel for a flake of MoS<sub>2</sub> with a thickness of a monolayer. The pixel was found with a threshold of 0.85 and a  $\Delta$  and  $\Psi$  range of  $\pm 2.2$ .

The region of the trilayer can be identified and located next to the area of the found monolayer of Graphene.

**The Graphene flake has a dimension of ca. 100  $\mu\text{m}$  x 20  $\mu\text{m}$ . Figure 6 demonstrates the capability to locate flakes with a size down to 10  $\mu\text{m}$ . The size of desired flakes or areas is limited to the lateral resolution and described by the clustersearch parameters. For the 3x3 pattern a monolayer flake of MoS<sub>2</sub> is found in a mapstack in the middle of the stitched image as seen in Figure 6.**

The ultraobjective is used to obtain a pattern for the MoS<sub>2</sub> flake. The ultraobjective is a Scheimpflug corrected optical system that provides an overall focused image. When using the ultraobjective a focus scan to obtain allover focused maps is no longer needed. That increases the speed of the measurement. The overall time for the 3x3 pattern with the ultraobjective was 20 min while the scanned area at an angle of incidence of 53° is around 1mm x 1mm.

### Conclusion

This application note shows the capability of spectroscopic imaging ellipsometry to automatically localize small flakes of Mono- to N-Layers of 2D materials. The method is independent from the substrate as well as from the experience of the user. It is also fast and provides information on the layer number with increased accuracy by using spectroscopic data. The algorithm is able to differentiate between a monolayer, bilayer and trilayer of graphene. Imaging ellipsometry also allows the localization of Molybdenum disulphide flakes with a size down to 10  $\mu\text{m}$ . A Scheimpflug corrected ultraobjective provides a speed increase in the recording of the pattern. However, the application is not limited to the localization of flakes of 2D materials. It is expandable to a wide range of thicknesses up to several microns of known transparent materials on known sample structures.

### References

- [1] K. S. Novoselov, A. K. Geim, S. V. Morozov, D. Jiang, Y. Zhang, S. V. Dubonos, I. V. Grigorieva, and A. A. Firsov, "Electric Field Effect in Atomically Thin Carbon Films," *Science*, vol. 306, no. 5696, pp. 666–669, Oct. 2004.
- [2] R. F. Frindt and A. D. Yoffe, "Physical properties of layer structures: optical properties and photoconductivity of thin crystals of molybdenum disulphide," *Proc. R. Soc. Lond. Ser. Math. Phys. Sci.*, vol. 273, no. 1352, pp. 69–83, 1963.
- [3] G.-H. Lee, Y.-J. Yu, X. Cui, N. Petrone, C.-H. Lee, M. S. Choi, D.-Y. Lee, C. Lee, W. J. Yoo, K. Watanabe, T. Taniguchi, C. Nuckolls, P. Kim, and J. Hone, "Flexible and Transparent MoS<sub>2</sub> Field-Effect Transistors on Hexagonal Boron Nitride-Graphene Heterostructures," *ACS Nano*, vol. 7, no. 9, pp. 7931–7936, Sep. 2013.
- [4] L. Britnell, R. M. Ribeiro, A. Eckmann, R. Jalil, B. D. Belle, A. Mishchenko, Y.-J. Kim, R. V. Gorbachev, T. Georgiou, S. V. Morozov, and others, "Strong light-matter interactions in heterostructures of atomically thin films," *Science*, vol. 340, no. 6138, pp. 1311–1314, 2013.
- [5] W. Choi, M. Y. Cho, A. Konar, J. H. Lee, G.-B. Cha, S. C. Hong, S. Kim, J. Kim, D. Jena, J. Joo, and others, "High-detectivity multilayer MoS<sub>2</sub> phototransistors with spectral response from ultraviolet to infrared," *Adv. Mater.*, vol. 24, no. 43, pp. 5832–5836, 2012.
- [6] K. Roy, M. Padmanabhan, S. Goswami, T. P. Sai, G. Ramalingam, S. Raghavan, and A. Ghosh, "A nearly relaxation-free optoelectronic memory from ultra-thin graphene-MoS<sub>2</sub> binary hybrids," *ArXiv Prepr. ArXiv13091455*, 2013.

[7] J. Qi, X. Li, X. Qian, and J. Feng, "Bandgap engineering of rippled MoS<sub>2</sub> monolayer under external electric field," *Appl. Phys. Lett.*, vol. 102, no. 17, p. 173112, 2013.

[8] V. G. Kravets, A. N. Grigorenko, R. R. Nair, P. Blake, S. Anissimova, K. S. Novoselov, and A. K. Geim, "Spectroscopic ellipsometry of graphene and an exciton-shifted van Hove peak in absorption," *Phys. Rev. B*, vol. 81, no. 15, p. 155413, 2010.

[9] U. Wurstbauer, C. Röling, U. Wurstbauer, W. Wegscheider, M. Vaupel, P. H. Thiesen, and D. Weiss, "Imaging ellipsometry of graphene," *Appl. Phys. Lett.*, vol. 97, no. 23, p. 231901, 2010.

[10] A. Matković, A. Beltaos, M. Miličević, U. Ralević, B. Vasić, D. Jovanović, and R. Gajić, "Spectroscopic imaging ellipsometry and Fano resonance modeling of graphene," *J. Appl. Phys.*, vol. 112, no. 12, p. 123523, 2012.

[11] I. Jung, M. Vaupel, M. Pelton, R. Piner, D. A. Dikin, S. Stankovich, J. An, and R. S. Ruoff, "Characterization of Thermally Reduced Graphene Oxide by Imaging Ellipsometry," *J. Phys. Chem. C*, vol. 112, no. 23, pp. 8499–8506, Jun. 2008.

[12] O. Albrektsen, R. L. Eriksen, S. M. Novikov, D. Schall, M. Karl, S. I. Bozhevolnyi, and A. C. Simonsen, "High resolution imaging of few-layer graphene," *J. Appl. Phys.*, vol. 111, no. 6, p. 064305, 2012.

[13] H. Fujiwara, *Spectroscopic ellipsometry: principles and applications*. Chichester, England; Hoboken, NJ: John Wiley & Sons, 2007.

[15] H. G. Tompkins and E. A. Irene, *Handbook of ellipsometry*. Norwich, NY; Heidelberg, Germany: William Andrew Pub. ; Springer, 2005.

[14] R. M. A. Azzam and N. M. Bashara, *Ellipsometry and polarized light*. Amsterdam; New York: North-Holland : Sole distributors for the USA and Canada, Elsevier Science Pub. Co., 1987.